Re-orientation of the easy axis in ϕ 0 -junction

Yu. M. Shukrinov, A. Mazanik, I. R. Rahmonov, A. E. Botha, Alexandre I. Buzdin

▶ **To cite this version:**

Yu. M. Shukrinov, A. Mazanik, I. R. Rahmonov, A. E. Botha, Alexandre I. Buzdin. Re-orientation of the easy axis in ϕ 0 -junction. EPL - Europhysics Letters, 2018, 122 (3), pp.37001 (1-5). 10.1209/0295-5075/122/37001 . hal-01845339

HAL Id: hal-01845339
https://hal.science/hal-01845339

Submitted on 20 Jul 2018

HAL is a multi-disciplinary open access archive for the deposit and dissemination of scientific research documents, whether they are published or not. The documents may come from teaching and research institutions in France or abroad, or from public or private research centers.

L'archive ouverte pluridisciplinaire **HAL**, est destinée au dépôt et à la diffusion de documents scientifiques de niveau recherche, publiés ou non, émanant des établissements d'enseignement et de recherche français ou étrangers, des laboratoires publics ou privés.

Distributed under a Creative Commons Attribution - NonCommercial - ShareAlike 4.0 International License

Re-orientation of the easy axis in φ_0-junction

Yu. M. Shukrinov[1,2,5], A. Mazanik[1,3], I. R. Rahmonov[1,4], A. E. Botha[5] and A. Buzdin[6,7]

[1] *BLTP, JINR - Dubna, Moscow Region, 141980, Russia*
[2] *Dubna State University - Dubna, Russia*
[3] *Moscow Institute of Physics and Technology - Institutsky lane 9, Dolgoprudny, Moscow region, 141700, Russia*
[4] *Umarov Physical Technical Institute, TAS - Dushanbe, 734063, Tajikistan*
[5] *Department of Physics, University of South Africa - Private Bag X6, Florida 1710, South Africa*
[6] *University Bordeaux, LOMA UMR-CNRS 5798 - F-33405 Talence Cedex, France*
[7] *Department of Materials Science and Metallurgy, University of Cambridge - CB3 0FS, Cambridge, UK*

PACS 74.50.+r – Tunneling phenomena; Josephson effects
PACS 85.25.-j – Superconducting devices
PACS 85.25.Cp – Josephson devices

Abstract – We study theoretically a dynamics of the φ_0-Josephson junction, with direct coupling between magnetic moment and Josephson current, which shows features reminiscent of a Kapitza pendulum. We find that, starting with the magnetization along the z-axis, the character of the magnetization dynamics changes crucially as a stable position of the magnetic moment $\vec{m}$ is realized between the z- and y-axes, depending on the values of the system parameters. Changes in critical current and spin-orbit interaction lead to different stability regions for the magnetization. Excellent agreement is obtained between analytical and numerical results at low values of the Josephson–to–magnetic-energy ratio.

A ferromagnet can exert a strong influence on a Josephson junction (JJ), particularly, the superconductor-ferromagnet-superconductor (SFS) JJ oscillates between 0- and π-junctions as the thickness of the ferromagnet increases [1–6]. In a closed superconducting loop with π-junction a spontaneous circulating current appears without applied magnetic flux [7]. A very special situation is possible when the weak link is a non-centrosymmetric magnetic metal with broken inversion symmetry like MnSi or FeGe. In this case, Rashba-type spin-orbit coupling leads to a general current-phase relation $j = j_c \sin(\varphi - \varphi_0)$, where φ_0 is proportional to the strength of the broken inversion symmetry magnetic interaction [8–10]. An important issue is that the φ_0-junction provides a mechanism for direct coupling between the suppercurrent (superconducting phase) and the magnetic moment.

The mechanical analog of a simple pendulum with applied torque is very useful to gain insight into the physics of Josephson devices [11]. Here we introduce another analog between the magnetic φ_0-junction and a pendulum with an oscillating point of suspension. A particle moving simultaneously in a permanent field and in a field oscillating with a high frequency, demonstrates a very interesting feature: new stability points appear at some parameters of the particle and fields [12,13]. The system in which this feature was first studied is called the Kapitza pendulum. Particularly, in a pendulum with a vibrating point of suspension (pivot point), the external sinusoidal force can invert the stability position of the pendulum [12,14,15]. In this case the bottom equilibrium position is no longer stable. Any tiny deviation from the vertical increases in amplitude with time. In the presence of a periodic drive, the unstable fixed point can become dynamically stable. Kapitza provided an analytical insight into the reasons for stability, by splitting the motion into "fast" and "slow" variables, and by introducing an effective potential. His result was first obtained in the high-frequency limit. By averaging the classical equations of motion over the fast oscillations of the drive, Kapitza found that the "upper" equilibrium point becomes stable for large enough driving amplitudes, while the "lower" point becomes unstable. Kapitza's pioneering work initiated the field of vibrational mechanics, and his method is used to describe periodic processes in a variety of different physical systems, ranging from atomic physics, plasma physics, to cybernetical physics (see [16–21] and references therein). In the nonlinear control theory the Kapitza pendulum is used as an example of a parametric

oscillator that demonstrates the concept of "dynamic stabilization".

In this paper we study the dynamics of a φ_0-junction with direct coupling between the magnetic moment and Josephson current [22,23]. We find that the application of an external voltage may lead to different stability regions for the magnetization, *i.e.*, Kapitza pendulum features in the φ_0-junction. Developing our previous approach [24], we investigate the effect of superconducting current on the dynamics of the magnetic moment. We show that, starting with magnetization along the z-axis, the character of the $\vec{m}$ dynamics changes crucially as a stable position of $\vec{m}$ develops between the z- and y-axes, depending on the parameters of the system.

The ac Josephson effect provides an ideal tool to study magnetic dynamics in a φ_0-junction. To realize the ac Josephson effect, we apply a constant voltage V to the φ_0-junction. In this case the superconducting phase varies with time, as $\varphi(t) = \omega_J t$, where $\omega_J = 2\,\mathrm{eV}/\hbar$ is the Josephson frequency [23,25]. The dynamics of the considered system is then described by the Landau-Lifshitz-Gilbert equation

$$\frac{\mathrm{d}\mathbf{M}}{\mathrm{d}t} = \gamma \mathbf{H}_{\mathit{eff}} \times \mathbf{M} + \frac{\alpha}{M_0}\left(\mathbf{M} \times \frac{\mathrm{d}\mathbf{M}}{\mathrm{d}t}\right), \qquad (1)$$

with effective magnetic field $\mathbf{H}_{\mathit{eff}}$ in the form [23]

$$\mathbf{H}_{\mathit{eff}} = \frac{K}{M_0}\left[\Gamma \sin\left(\omega t - \varphi_0\right)\widehat{\mathbf{y}} + \frac{M_z}{M_0}\widehat{\mathbf{z}}\right], \qquad (2)$$

where γ is the gyromagnetic ratio, α is the phenomenological damping constant, $M_0 = \|\mathbf{M}\|$, and M_i are the components of $\mathbf{M}$. Below we use the normalized components $m_i = \frac{M_i}{M_0}$. Furthermore, $\varphi_0 = r\frac{M_y}{M_0}$, $r = l v_{so}/v_F$, $l = 4hL/\hbar v_F$, L is the length of the F-layer, h is the exchange field of the F layer, $\Gamma = Gr$, $G = E_J/(K\mathcal{V})$, and $E_J = \Phi_0 I_c/2\pi$ is the Josephson energy. Here Φ_0 is the flux quantum, I_c is the critical current, v_F is the Fermi velocity, and the parameter v_{so}/v_F characterizes a relative strength of spin-orbit interaction, while K is the anisotropic constant, and $\mathcal{V}$ is the volume of the F layer. To investigate the dynamics of considered system numerically, we write eq. (1) in the dimensionless form (see system of equations (1) in the Supplementary Material `Supplementarymaterial.pdf` (SM)). In that system the time is normalized to the inverse ferromagnetic resonance frequency $\omega_F = \gamma K/M_0 : (t \to t\omega_F)$, so ω is normalized to the ω_F.

First we present results of numerical simulations of the system (1) and (2). Figure 1 shows the dynamics of the magnetization components m_z and m_y at different values of the parameter G, demonstrating the re-orientation of the oscillations around the z-axis to the oscillations around the y-axis. With increase in G, the component m_y goes from zero to $m_y = 1$.

Figure 1(a) demonstrates the time dependence of m_z at $G = 5\pi$. The character of oscillations in the beginning and in the middle of time interval is shown in the insets. We see that the average value of m_z deviates from one. Figure 1(b) shows the corresponding oscillation of m_y. Figure 1(c) shows a stabilization of m_y oscillations around some average value of m_y, between the z- and y-directions with increase in G, *i.e.*, it shows the re-orientation of the oscillations at three values of $G = 10\pi, 20\pi, 50\pi$. With an increase in G, the time of re-orientation from the z-direction to the y-direction decreases substantially. At a sufficiently large value of G, the average value of m_y becomes close to 1, as we see in fig. 1(c), for case $G = 50\pi$. The oscillations show periodically splashing related to the Josephson frequency. The inset demonstrates the jumps of m_y from the value $m_y = 1$ with Josephson frequency. The amplitudes of the jumps decrease in time, becoming smaller and shorter in time, with an increase in G.

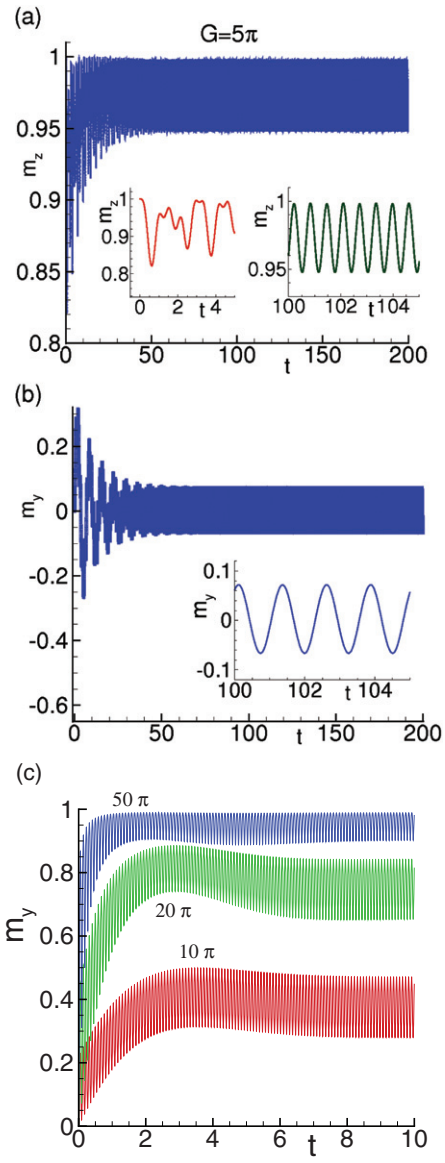

Fig. 1: (Color online) (a) Dynamics of the m_z component at $G = 5\pi$, $r = 0.1$; (b) the same for m_y; (c) effect of G at $r = 0.5$. The numbers show the G value.

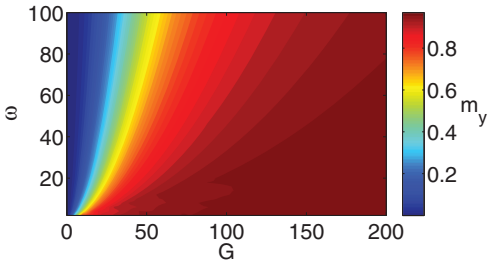

Fig. 2: (Color online) The ω-G diagram for averaged m_y shown by the color scale.

We note that the effect of r leads to similar features as we observe for changes in G. So, the situation is reminiscent of the Kapitza pendulum, *i.e.*, a pendulum whose point of suspension vibrates, leading to the inversion of the stability positions of the pendulum [12].

Variation of average m_y as a function of frequency ω and G is shown in fig. 2. We see that an increase in G makes orientation of m_y along the y-axis stable, but that the frequency dependence differs from the characteristic Kapitza pendulum behavior, as we can see in fig. 4. The system of equations (1), describing the dynamics of the magnetic moment in the angular variables $m_z = \cos\theta$, $m_x = \sin\theta\cos\phi$, $m_y = \sin\theta\sin\phi$, can be written as

$$\begin{cases} \dot{\phi} = \dfrac{\cos\theta}{1+\alpha^2} \\ -\dfrac{Gr}{1+\alpha^2}\dfrac{1}{\sin\theta}\left[\cos\theta\sin\phi - \alpha\cos\phi\right]\sin\left[\omega\tau - r\sin\theta\sin\phi\right], \\ \dot{\theta} = -\dfrac{\alpha\sin 2\theta}{2(1+\alpha^2)} \\ +\dfrac{Gr}{1+\alpha^2}\left[\alpha\cos\theta\sin\phi + \cos\phi\right]\sin\left[\omega\tau - r\sin\theta\sin\phi\right]. \end{cases} \tag{3}$$

In the case of no coupling between the magnetic moment and the Josephson junction, at $G = 0$, we have

$$\begin{cases} \dot{\phi} = \dfrac{\cos\theta}{1+\alpha^2}, \\ \dot{\theta} = -\dfrac{\alpha\sin 2\theta}{2(1+\alpha^2)}. \end{cases} \tag{4}$$

The solution to eq. (4) has the form

$$\theta(\tau) = \mathrm{ArcTan}\left[\exp\left\{\log\tan\theta_0 - \frac{\alpha\tau}{1+\alpha^2}\right\}\right], \tag{5}$$

where $\tan\theta_0$ is considered to be positive for simplicity. So, the characteristic scale in time to order the magnetic moment along the easy axes is $\tau^\star = \frac{1+\alpha^2}{\alpha}$. To realize the Kapitza pendulum we should investigate the case $\omega \gg \frac{2\pi}{\tau^\star} = \frac{2\pi\alpha}{1+\alpha^2}$, where ω is the frequency of the external fast-varying field.

Let us make the replacements

$$\begin{aligned} \theta &\to \Theta + \xi, \\ \phi &\to \Phi + \eta. \end{aligned} \tag{6}$$

Here Θ and Φ describe slow movement, while ξ and η are coordinates for fast-varying movement. Conditions for ξ and η are discussed in the SM. We consider $\overline{\theta} = \Theta$, $\overline{\phi} = \Phi$, where averaging is taken over the period of the fast-varying force $T = \frac{2\pi}{\omega}$.

The system of equations for slow movement has a form (see SM)

$$\begin{cases} \dot{\Phi} = \dfrac{\cos\Theta}{1+\alpha^2} - \dfrac{(Gr)^2 r\alpha}{2\omega(1+\alpha^2)^2}\cdot\dfrac{1}{\sin\Theta}\left[\cos\Theta\sin\Phi\right. \\ \qquad \left. -\alpha\cos\Phi\right]\left\{1-\sin^2\Theta\sin^2\Phi\right\}, \\ \dot{\Theta} = -\dfrac{\alpha\sin 2\Theta}{2(1+\alpha^2)} + \dfrac{(Gr)^2 r\alpha}{2\omega(1+\alpha^2)^2}\left[\alpha\cos\Theta\sin\Phi\right. \\ \qquad \left. +\cos\Phi\right]\left\{1-\sin^2\Theta\sin^2\Phi\right\}. \end{cases} \tag{7}$$

There are some equilibrium points of the system following from $\dot{\Theta} = 0, \dot{\Phi} = 0$.

The first pair is located on the equator

$$\Theta_0 = \pi/2, \quad \Phi_0 = \pi/2 \text{ and } \Theta_0 = \pi/2, \quad \Phi_0 = 3\pi/2. \tag{8}$$

Linearization of (7) after substitution $\Phi = \Phi_0 + \delta\phi, \Theta = \Theta_0 + \delta\theta$ gives

$$\begin{cases} \dot{\delta\phi} = \dfrac{1}{1+\alpha^2}\delta\theta, \\ \dot{\delta\theta} = \dfrac{\alpha}{1+\alpha^2}\delta\theta. \end{cases} \tag{9}$$

It is clear that $\delta\theta \sim e^{\frac{\alpha\tau}{1+\alpha^2}}$, so these points are unstable.

Using (7) we find that the equilibrium points at $\Phi_0 = \frac{\pi}{2}$ are described by equation

$$\sin\Theta_0 = \frac{-1+\sqrt{1+4\beta^2}}{2\beta}, \tag{10}$$

where $\beta = \frac{(Gr)^2 r\alpha}{2\omega(1+\alpha^2)}$, which can be approximated as $\sin\Theta_0 = \beta$ at small β. It has two solutions in the interval $0 \le \Theta_0 \le \pi$. Note that at $\Phi_0 = \frac{3\pi}{2}$ we have $\sin\Theta_0 = \frac{1-\sqrt{1+4\beta^2}}{2\beta}$ which leads to the negative $\sin\Theta_0$, but Θ is always positive. So, there are not any stable points at $\Phi_0 = \frac{3\pi}{2}$.

To find out if these points are stable we have linearized eq. (7) near the points, and tested the eigenvalues of the linearized system. This straightforward calculation shows that the real parts of eigenvalues of the corresponding system are always negative. It means that the second pair of points are always stable (see SM). Figure 3 shows the location of the unstable and stable pairs of equilibrium points.

Results of numerical calculations of the averaged m_y as a function G at different frequencies are presented in fig. 4. We see that system reminiscent the Kapitza pendulum behavior: the averaged m_y component characterizing changes of stability direction is growing with G. The character of behavior depends essentially on the frequency of the fast-varying field getting very sharp at small ω. Figure 4 also compares the $m_y(G)$ dependence obtained by analytical and numerical calculations. We see results

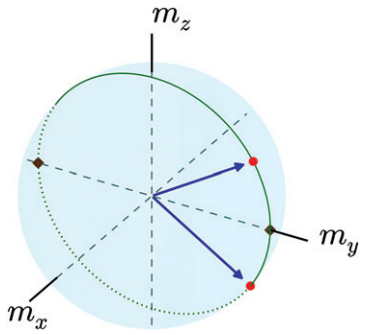

Fig. 3: (Color online) Demonstration of the equilibrium points of eq. (7). Arrows show stable points, the other two points are unstable.

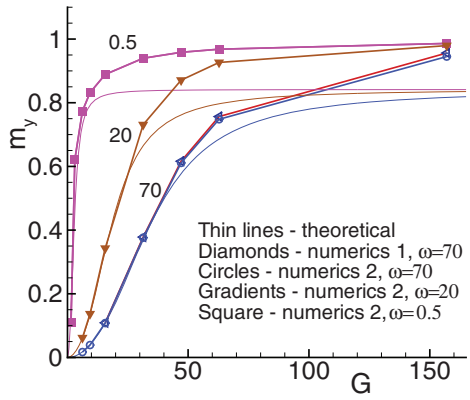

Fig. 4: (Color online) Comparison of the data of theoretical and numerical calculations for G-dependence of the averaged m_y at different frequencies and $r = 0.5$ and $\alpha = 1$. Thin lines show theoretical G-dependence of m_y according to formula (10). Symbols show numerical results, thick lines guide the eyes.

at three frequencies: $\omega = 0.5$, 20 and 70. The analytical dependence is calculated according to formula (10). Two methods are used for numerics: numerics-1 is based on the standard program "Mathematica" (shown by triangles, calculated for $\omega = 70$) and numerics-2 presents results of the direct solution of system (1) based on the Runge-Kutta fourth order. Both numerics give practically the same results. An excellent agreement between analytical and numerical results is obtained at low G, depending on the frequency of the fast-varying field. For high frequencies the coincidence is still good at rather large G.

Table 1 shows the values of the averaged m_y obtained by analytic and numerical calculations at different G. The difference in values of the averaged m_y obtained by all the three used methods is rather small. There is an essential difference between the original Kapitza pendulum and our system. In the Kapitza pendulum the stability of a new equilibrium point is determined by the amplitude and frequency of the external force. In our case, two new points are always stable and their positions on the unit sphere is determined by the parameters of the system.

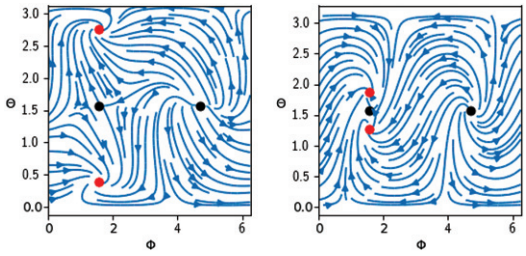

Fig. 5: (Color online) Phase planes (7) at $G = 10\pi$ (left) and $G = 50\pi$ (right). Here $r = 0.5$, $\alpha = 1$, $\omega = 70$. Red points are stable equilibrium points which are calculated from (10), black points are unstable (8). With increase in G the stable red points are approaching unstable ones $\Phi_0 = \pi/2$, $\Theta_0 = \pi/2$.

Table 1: m_y from the theory and the numerical results.

G	Θ_0	analytic m_y	numerics-1	numerics-2
15.7	1.462	0.109	0.108	0.109
31.4	0.387	0.369	0.376	0.378
47.1	0.663	0.577	0.611	0.616
62.8	0.859	0.689	0.748	0.756
157	1.272	0.817	0.945	0.956

Figure 5 shows the vector fields in the plane $0 \le \Phi \le 2\pi$, $0 < \Theta < \pi$ according to eq. (7) at two different values of G: 5π and 50π. This demonstrates that with an increase in G the two equilibrium positions approach the unstable point at $\Phi = \frac{\pi}{2}$, $\Theta = 0$. This result is in agreement with (10), which shows that an increase in G leads to an increase in β, and to the convergence of $\sin\Theta_0$ to one.

There is another interesting phenomenon which is realized in our case. With changing parameters of the system, the stable equilibrium positions of the "slow" movement are approaching the unstable one at $\Phi = \frac{\pi}{2}$, $\Theta = \pi/2$. When the distance between them becomes comparable to the amplitude of the "fast" motion, all the three special points of the "slow" system effectively merge.

Finally, we specify the set of ferromagnetic layer parameters and junction geometry that make it possible to reach the values used in our numerical calculations, for the possible experimental observation of the predicted effect. In our model the interaction between the Josephson current and the magnetization is determined by the parameter $G = E_J/K * V$, which describes the ratio between the Josephson energy and the magnetic anisotropy energy. To have a strong interaction, one needs to choose a ferromagnet with weak magnetic anisotropy, like, for example, the permalloy with $K \sim 4 * 10^{-5}\,\mathrm{K\AA}^{-3}$ [26], and a junction with a relatively high critical current. Recently, a high critical current density of $(3 * 10^5 – 5 * 10^6)\,\mathrm{A/cm^2}$ was reported for a Nb/NiGdNi/Nb junction [27]. For the volume $\mathcal{V}$ of the ferromagnetic film $\mathcal{V} = 10^{-15}\,\mathrm{cm}^3$ ($10^{-5}\,\mathrm{cm} \times 10^{-4}\,\mathrm{cm} \times 10^{-6}\,\mathrm{cm}$), we find $G \sim 20$–200, for these parameters.

The strength of the specific Rashba-type spin-orbit interaction in our case is controlled by the parameter

$\Gamma = Gr$, which should be stronger in metals with large atomic number Z. A suitable candidate may be a permalloy doped with Pt [28]. In Pt the spin-orbit interaction plays a crucial role in electronic band formation and the parameter $v_{so}/v_F \sim 1$. The doping of the permalloy by Pt, up to 10 percent, did do not change the magnetic properties significantly, and therefore we may expect to have $v_{so}/v_F \sim 0.1$, in this case. If the length of the ferromagnetic layer is of the order of the magnetic decaying length, *i.e.*, $l \sim 1$, we have $r \sim 0.1$, the value of the parameter Γ is in the range 2–20. Note that ferromagnets without inversion symmetry, like MnSi or FeGe, may also be interesting candidates for the observation of the discussed phenomena.

In conclusion, we have demonstrated that the direct coupling between the magnetic moment and Josephson current in a φ_0-junction may effectively lead to strong re-orientation of the magnetic easy axis in response to an applied voltage. This serves as a manifestation of Kapitza-like pendulum behavior and opens a new way to control the magnetization via a superconducting current.

* * *

The authors thank K. Sengupta, K. Kulikov, I. Bobkova, and A. Bobkov for useful discussions. The study was partially funded by the RFBR (research project 18-02-00318), and the SA-JINR Collaborations. YuMS and AEB gratefully acknowledge support from the University of South Africa's visiting researcher program. AB acknowledges the French ANR projects "SUPERTRONICS" and Leverhulme Trust for supporting his stay in Cambridge.

REFERENCES

[1] Ryazanov V. V., Oboznov V. A., Rusanov A. Yu., Veretennikov A. V., Golubov A. A. and Aarts J., *Phys. Rev. Lett.*, **86** (2001) 2427.
[2] Oboznov V. A., Bol'ginov V. V., Feofanov A. K., Ryazanov V. V. and Buzdin A. I., *Phys. Rev. Lett.*, **96** (2006) 197003.
[3] Robinson J. W. A., Piano S., Burnell G., Bell C. and Blamire M. G., *Phys. Rev. Lett.*, **97** (2006) 177003.
[4] Linder J. and Robinson J. W. A., *Nat. Phys.*, **11** (2015) 307.
[5] Mai S., Kandelaki E., Volkov A. F. and Efetov K. B., *Phys. Rev. B*, **84** (2011) 144519.
[6] Cai L., Garanin D. A. and Chudnovsky E. M., *Phys. Rev. B*, **87** (2013) 024418.
[7] Bulaevskii L. N., Kuzii V. V. and Sobyanin A. A., *JETP Lett.*, **25** (1977) 314.
[8] Buzdin A., *Phys. Rev. Lett.*, **101** (2008) 107005.
[9] Krive I. V., Kadigrobov A. M., Shekhter R. I. and Jonson M., *Phys. Rev. B*, **71** (2005) 214516.
[10] Reynoso A. A., Usaj G., Balseiro C. A., Feinberg D. and Avignon M., *Phys. Rev. Lett.*, **101** (2008) 107001.
[11] Antonio Barone and Gianfranco Paternò, *Physics and Applications of the Josephson Effect* (John Wiley and Sons Inc.) 1982.
[12] Kapitza P. L., *Soviet Phys. JETP*, **21** (1951) 588; *Usp. Fiz. Nauk*, **44** (1951) 7.
[13] Landau L. D. and Lifshitz E. M., *Mechanics*, Vol. **1**, 1st edition (Pergamon Press) 1960, ASIN B0006AWV88.
[14] Lev P. Pitaevskii, *Phys.-Usp.*, **54** (2011) 625.
[15] Butikov Eugene I., *J. Phys. A: Math. Theor.*, **44** (2011) 295202.
[16] Citro Roberta, Dalla Torre Emanuele G., D'Alessio Luca, Polkovnikov Anatoli, Babadi Mehrtash, Oka Takashi and Demler Eugene, *Ann. Phys.*, **360** (2015) 694.
[17] Boukobza Erez, Moore Michael G., Cohen Doron and Vardi Amichay, *Phys. Rev. Lett.*, **104** (2010) 240402.
[18] Longhi S., *EPL*, **118** (2017) 20004.
[19] Shayak B., *EPL*, **118** (2017) 45002.
[20] Martin J., Georgeot B., Gury-Odelin D. and Shepelyansky D. L., *Phys. Rev. A*, **97** (2018) 023607.
[21] Fialko O., Opanchuk B., Sidorov A. I., Drummond P. D. and Brand J., *EPL*, **110** (2015) 56001.
[22] Buzdin A. I., *Rev. Mod. Phys.*, **77** (2005) 935.
[23] Konschelle F. and Buzdin A., *Phys. Rev. Lett.*, **102** (2009) 017001.
[24] Shukrinov Yu. M., Rahmonov I. R., Sengupta K. and Buzdin A., *Appl. Phys. Lett.*, **110** (2017) 182407.
[25] Josephson B. D., in *Superconductivity*, edited by Parks R. D., Vol. **1** (Marcel Dekker, New York) 1968, Chapt. 9.
[26] Rusanov A. Yu., Hesselberth M., Aarts J. and Buzdin A. I., *Phys. Rev. Lett.*, **93** (2004) 057002.
[27] Robinson J. W. A., Chiodi F., Egilmez M., Halász G. B. and Blamire M. G., *Sci. Rep.*, **2** (2012) 699.
[28] Hrabec A., Goncalves F. J. T., Spencer C. S., Arenholz E., N'Diaye A. T., Stamps R. L. and Marrows C. H., *Phys. Rev. B*, **93** (2016) 014432.